

The influence of friction stir welding parameters on the mechanical properties and low cycle fatigue in AA 6063 (AlMgSi0.5) alloy

S. Sayer*, V. Ceyhun, Ö. Tezcan

Department of Mechanical Engineering, Engineering Faculty, Ege University, 35100 Bornova, İzmir, Turkey

Received 28 August 2007, received in revised form 1 February 2008, accepted 14 February 2008

Abstract

In this study, AA 6063 (AlMgSi0.5) aluminium alloy plates were welded by friction stir welding, a solid state welding procedure. The aim of this study is to investigate the influence of the process parameters on the microstructure, mechanical properties and low cycle fatigue behaviour of this particular alloy. Three different rotation and welding speeds have been selected, which makes a total of nine different welding conditions. Depending on the welding parameters, void-free and void containing welds have been obtained. A great majority of the specimens have broken in the region between the HAZ and the TMAZ. The weld mechanical properties are observed to be about 70 % of those of the base metal. About a 40 % decrease has been detected in welded specimens in terms of low cycle fatigue life.

Key words: friction stir welding, aluminium alloy AA 6063, rotation speed, welding speed, low cycle fatigue, mechanical properties

1. Introduction

Friction stir welding (FSW) is a newly developed method of joining materials compared to conventional welding techniques, patented by the Welding Institute (TWI) in 1991. FSW technology is being widely considered by modern aerospace, shipbuilding and automotive industries for high performance structural demand [1–5].

The process operates by generating frictional heat between a rotating tool of harder material than the workpiece being welded, in such a manner as to thermally condition the abutting weld region in the softer material. The tool is shaped with a larger diameter shoulder and a smaller diameter pin, which is specially profiled [6]. This process constitutes a development of the classical friction welding methods. In the FSW process, no melting of the joining parts occurs and the weld forms through solid-state plastic flow at elevated temperature. FSW offers the advantage of reduced porosity, distortion and residual stresses if the welding parameters are correctly optimized, which are typical defects encountered in the

fusion processes. Moreover, consumable filler material, shielding gas and edge preparation are normally not necessary [6, 7].

On the other hand, problems encountered in FSW include insufficient weld joint when welding is carried one-sided; in this case double-sided welding may be offered. Also FS welding of thin materials (< 1.25 mm) may not be effective due to lack of stirring and inadequate heat input.

The simultaneous rotational and translational motion of the welding tool during the welding process creates a characteristic asymmetry between the adjoining sides. The side where the tool rotation coincides with the direction of the translation of the welding tool is called the advancing side (AS), while the other side, where the two motions, rotation and translation counteract is called the retreating side (RS) [8, 9]. A schematic description of the friction stir process conducted for AA 6063 is presented in Fig. 1.

In contrast to traditional friction welding, which is usually performed on small asymmetric parts that can be rotated and pushed against each other to form a joint, FSW can be applied to various types of joints

*Corresponding author: tel.: +90 232 343 66 00 ext. 7026; fax: +90 232 388 75 99; e-mail address: sami.sayer@ege.edu.tr

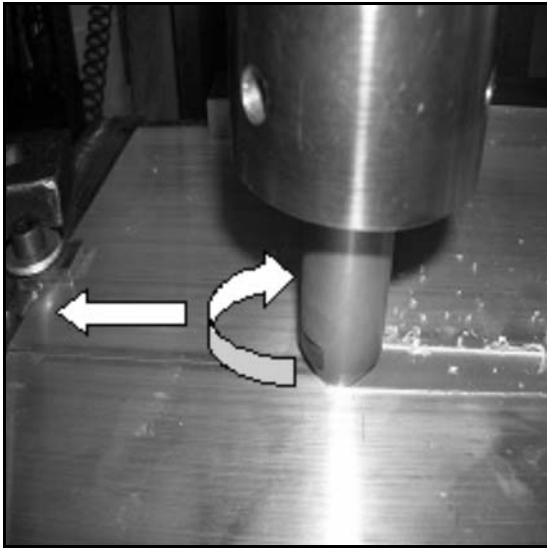


Fig. 1. FSW technology schematic view.

like butt joints, lap joints, T-butt joints, and fillet joints [10, 11].

The difficulty of making high-strength, fatigue and fracture resistant welds in aerospace aluminium alloys, such as highly alloyed 2xxx and 7xxx series, has long inhibited the wide use of welding for joining aerospace structures. These aluminium alloys are generally classified as non-weldable because of the poor solidification microstructure and porosity in the fusion zone. Also, the loss in mechanical properties as compared to the base material is very significant. These factors make the joining of these alloys by conventional welding processes unattractive. Some aluminium alloys, like AA 6063, can be resistance welded, but the surface preparation is expensive, with surface oxide being a major problem. Therefore, the first trials on the FSW of aluminium alloys have started on the 2xxx and 7xxx series, followed by 5xxx and 6xxx series due to the advantages supplied by the FSW process.

FSW of aluminium alloys offers the advantages of low heat input, reduced distortion, therefore low residual stresses and higher mechanical properties compared to conventional fusion welding methods. Owing to these advantages, FS welded aluminium alloys are widely used in commercial transportation systems and in aerospace industry, where reduced fuel consumption is of vital importance.

Al 6063 is a light alloy widely used in the transport and construction industries, namely in truck and train bodies and exterior siding, due to its high corrosion resistance, heat treatability, weldability and cold-forming properties.

Although existing literature includes studies on the influence of welding parameters on the joint properties of Al alloys, no specific study has been found on AA

Table 1. Chemical composition of AA 6063 (wt.%)

Mg	Si	Fe	Mn	Ti	Cu	Others	Al
0.52	0.46	0.16	0.019	0.012	0.006	0.32	balance

6063, except that Sato et al. have examined the influence of solution heat treatment ageing on the mechanical properties of FS welded 4 mm thickness 6063 alloy, using constant welding speed of 360 mm min^{-1} with varying rotation speeds [12].

In this study, the influence of varying welding and rotation speeds on the microstructure, mechanical properties and low cycle fatigue behaviour of FS welded AA 6063 alloy has been examined using a specifically developed tool for the welding process. There is ongoing research on the effect of tool design on the microstructural and mechanical properties of AA 6063. These will be presented in a future work.

2. Material and experimental procedures

2.1. Material

The material was produced as extruded flat plate, with dimensions of $275 \times 150 \times 5 \text{ mm}$ (length, width, thickness). The chemical composition of aluminium alloy 6063 is given in Table 1.

2.2. Friction stir welding

FSW was carried out on 5 mm thick Al 6063 plates. The welding direction was taken such that it was aligned with the rolling direction of the plate. Three levels of tool rotation speed (900, 1600 and 2800 rpm) and three levels of welding speed ($100, 200$ and 400 mm min^{-1}), making a total of nine conditions, were selected after various trials to determine the most effective range of welding parameters. The variation of these parameters is shown in Fig. 2. In this figure, condition A refers to a welding speed of 100 mm min^{-1} and a rotation speed of 900 rpm, condition B refers to a welding speed of 100 mm min^{-1} and a rotation speed of 1600 rpm. From here on letters A to I will be used to indicate the welding conditions.

FSW tool was used with a threaded conical pin (5 mm base and 4.5 mm head diameter), a pin length of 4.6 mm, and a shoulder diameter of 15 mm. Tool configuration is given in Fig. 3. The FSW tool was fixed to the rotating axis of a CNC machine in the clockwise direction. The tool was tilted slightly from the outer normal of the plate. The tilt angle was set to 3° to the outer normal of the plane of the plates. The plates were prepared so as to measure the temperature at two points, namely, on advancing (AS) and re-

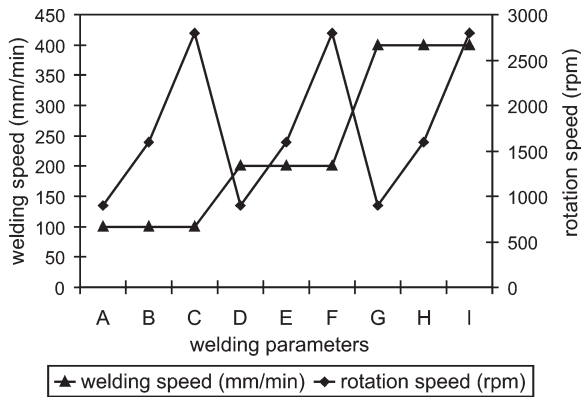


Fig. 2. Welding parameters.

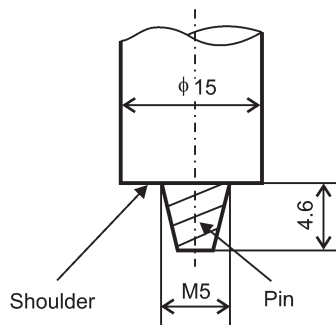


Fig. 3. Tool configuration.

treating sides (RS) using thermocouples. The K-type thermocouples of 1 mm diameter were subsequently inserted into the holes drilled at the mid-length of the plates, 10 mm from the edges to be welded, and glued so that the thermocouple ends were in intimate contact with the workpiece.

Standard transverse tensile and fatigue specimens were cut out from the welded plates, which are prepared according to ASTM E 8-95a for tensile testing and ASTM E 466 for fatigue testing [13]. In all of the plates, specimens were extracted perpendicular to the welding direction.

3. Results and discussion

As expected, with a lower welding speed (100 mm min^{-1}) and higher rotation speed (1600 rpm and 2800 rpm), the amount of heat supplied to the material was greater. Many researchers have indicated that the temperature distribution during FSW constitutes an important factor in terms of the weld strength and microstructure of the nugget zone. Most of the research on this topic has been centered on the temperature distribution in a specific area rather than the comparison of different areas. In this study the temperature differ-

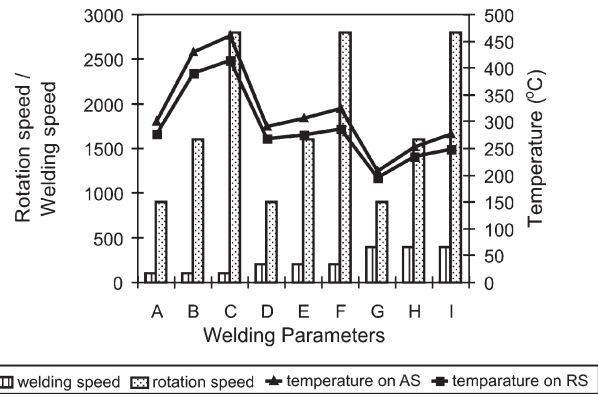


Fig. 4. Measured temperature of the plate during FSW as a function of different welding parameters.

ence between the AS and RS sides has been considered for the different welding parameters. The temperature variation according to differing welding parameters is given in Fig. 4. As can be seen in the figure, the measured temperature on the AS side is greater compared to that on the RS side. The explanation for this can be related to the grain sizes obtained at the AS and RS sides. It has been observed that the average grain size within the weld zone tends to increase near the top of the weld zone and decreases with distance on either side of the weld zone centreline and this corresponds roughly to temperature variation within the weld zone [14–16]. Furthermore, the average grain size at the AS has been found to be greater compared to the RS. For example it has been reported that while the average grain size at AS was about $5.1 \mu\text{m}$, it was about $3.5 \mu\text{m}$ at the RS [17].

Further research is underway on the influence and distribution of temperature on the weld microstructure and weld parameters.

3.1. Microstructure

The transverse macro-sections reveal the characteristic features of FSWs in Al alloys. The joint region is divided into a thermo-mechanically affected zone (TMAZ) and heat affected zone (HAZ). The part of the TMAZ that experiences high strain and undergoes recrystallization is called the nugget zone (NZ). Figure 5 illustrates the zones of a FSW joint in the Al alloy used in this study. Studies have shown that the weld nugget is composed of fine equiaxed grains which are formed under high temperature and plastic deformation in the weld centre due to the stirring process [18]. The TMAZ is the region surrounding the nugget on either side where there is less heat generation compared to the weld centre [19].

After welding, the joints were cross-sectioned perpendicular to the welding direction and specimens were extracted for metallographic analysis and

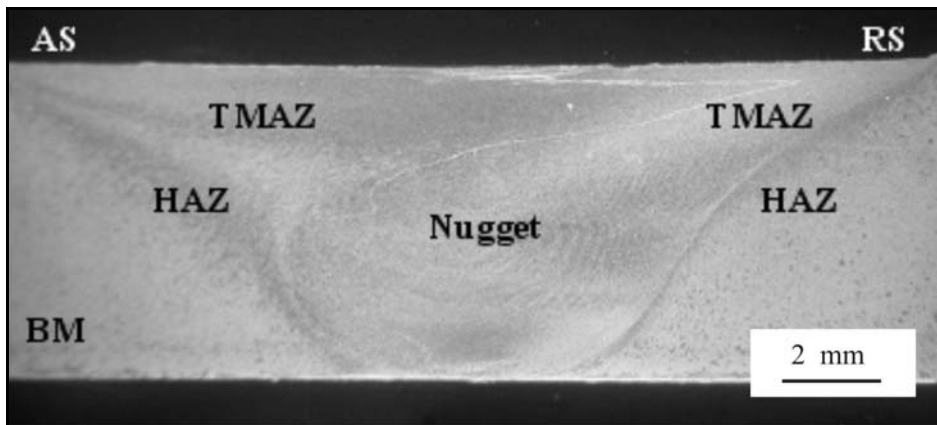


Fig. 5. Cross-section of a FSW joint; (BM) Base Material, (HAZ) Heat Affected Zone, (TMAZ) Thermo-Mechanically Affected Zone, Nugget.

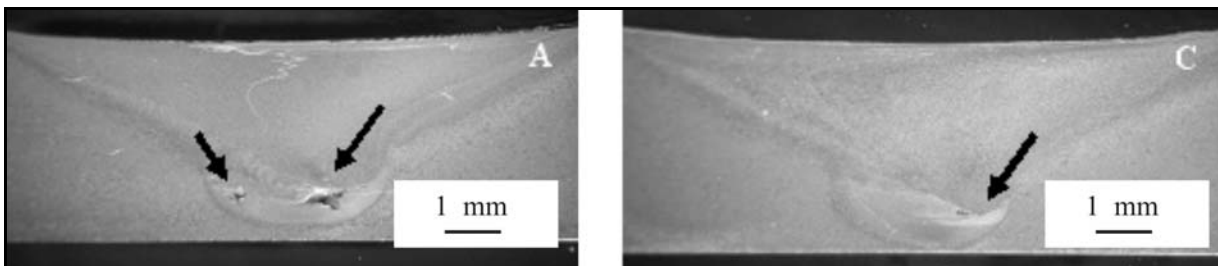


Fig. 6. Macrostructure of the weld cross-section of 6063 alloy for two welding parameters (A: 900 rpm, 100 mm min⁻¹; C: 2800 rpm, 100 mm min⁻¹).

tensile tests using an electrical-discharge cutting machine. The cross-sections of the metallographic specimens were polished with alumina suspension, etched with Keller's reagent (1.5 ml HCl, 2.5 ml NHO₃, 1 ml HF, 95 ml H₂O) for about 30 s, and observed by optical microscopy. The microstructural features of the welds were investigated on an optic microscope. The onion ring structure of the nugget zone was easily detectable at welding parameters of 1600 rpm rotation speed and 100 and 200 mm min⁻¹ welding speeds, while for other parameters it was not so clear.

At low rotation (900 rpm) and high welding speeds (400 mm min⁻¹), a porous structure was observed at the lower portion of the nugget zone. The porous structures at the lower nugget zone did not only result from the welding parameters but also from the conical shape of the pin construction. Therefore, the slender tip of the pin was insufficient to stir the material, causing cavities to occur. The macrostructure of the weld cross-section of 6063 alloy for two welding parameters is given in Fig. 6. At low rotation speed of 900 rpm, due to insufficient heat input, a porous structure and an incomplete welding corresponding to about 10 % material thickness were observed. Whereas at a high rotation speed of 2800 rpm, a nearly complete weld is obtained with less porosity compared to the low rotation speed of

900 rpm.

It has been seen that after the welding procedure, the grain structure has refined due to re-crystallization and that the grains were oriented. The macro- and micro-sections of the weld cross-section are given in Fig. 7.

3.2. Microhardness

Microhardness measurements were carried out across the weld zone. Measurements were performed under a load of 80 g for 10 s. Figure 8 shows the microhardness distribution over the weld cross-section of 6063 aluminium alloy. The welding process softens the material around the weld line and reduces the hardness. But the nugget hardness recovery is due to re-crystallization of a very fine grain structure. Therefore the centre of weld nugget was significantly harder than the thermo-mechanically affected region immediately outside the nugget boundary. There was a hardness decrease at the HAZ region, as expected, due to the differences in the grain size.

3.3. Tensile testing

The tensile tests were carried out at room temperature at a crosshead speed of 1 mm min⁻¹ using a

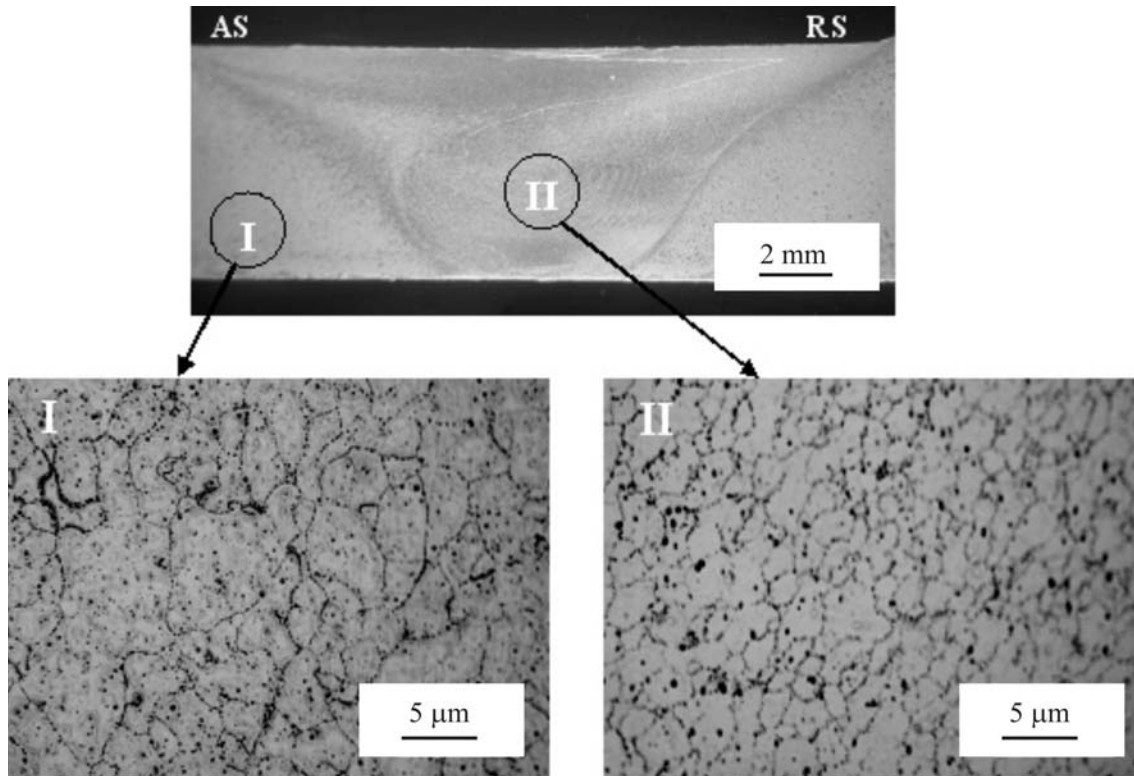


Fig. 7. Macro- and microstructure of welding specimens (A: 1600 rpm, 100 mm min⁻¹).

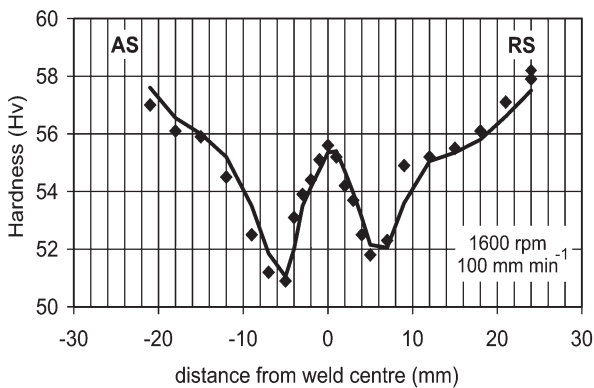


Fig. 8. Microhardness distribution over the weld cross-section by the condition B (rotation speed 1600 rpm, welding speed 100 mm min⁻¹).

computer-controlled testing machine. The specimens were cut perpendicular to the welding direction. The specimen geometry in mm is given in Fig. 9. In this figure, L_0 is the gauge length, which includes the nugget zone, TMAZ and HAZ on both sides.

Specimens welded at 1600 rpm broke on the advancing side at the intersection between the TMAZ and the HAZ, while specimens welded at high welding and low rotation speeds that contain porosity were broken at the nugget zone. The tensile properties of base material (BM) and welded specimens are given in

Fig. 10. The values are average of at least three tests. The maximum tensile strength was obtained in specimens with rotation speeds of 1600 and 2800 rpm and a welding speed of 100 mm min⁻¹. Yield strength values of the welded specimens are much lower than the yield strength of the BM (about 40 % of the BM value). It has been seen that variation of the weld parameters did not significantly affect the yield strength.

3.4. Low cycle fatigue testing

Low cycle fatigue tests are carried out at a comparatively high stress and frequency of stress variation. Only porosity-free specimens (B, E and G) were included in the fatigue testing. The low cycle fatigue tests were performed on a servo-hydraulic test machine with as-welded specimens. The specimen was cut perpendicular to the weld axis. The length L_0 (36 mm) includes the weld nugget, TMAZ and HAZ and the base metal on both sides. Figure 11 shows the schematic of a fatigue specimen.

During the tests the material was damaged by elastic-plastic straining. The mean stress was 80 MPa in all tests, which was beyond the yield strength values of the welded specimens. The tests were performed under stress control (keeping the mean stress constant for three $R = \sigma_{\min}/\sigma_{\max}$ ratios) and a constant stroke rate of 1 mm min⁻¹, with a working frequency of 10 Hz. The three stress ratios used in the tests are $R_1 =$

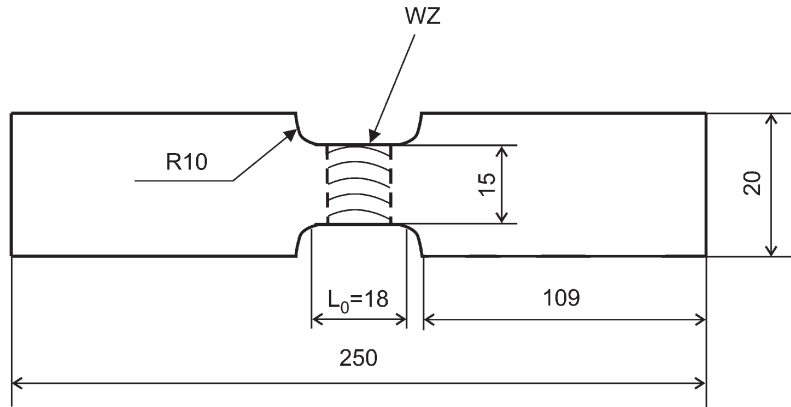


Fig. 9. Tensile specimen geometry.

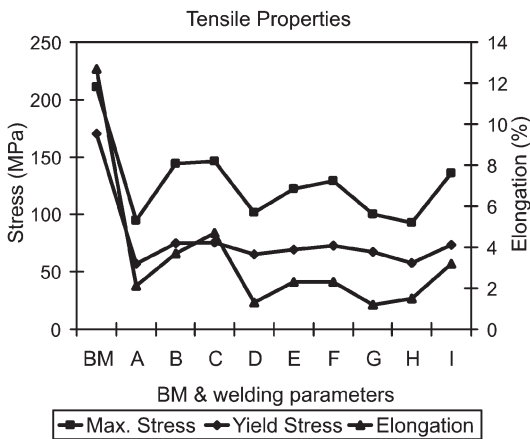


Fig. 10. The tensile properties of BM and of specimens of various welding parameters.

0.33 ($\sigma_{\min} = 40 \text{ MPa}/\sigma_{\max} = 120 \text{ MPa}$), $R_2 = 0.23$ ($\sigma_{\min} = 30 \text{ MPa}/\sigma_{\max} = 130 \text{ MPa}$), $R_3 = 0.14$ ($\sigma_{\min} = 20 \text{ MPa}/\sigma_{\max} = 140 \text{ MPa}$). All the tests were conducted until failure.

It was seen that the welded specimens were broken

at the nugget zone. The test results are given in Fig. 12. Stress amplitude, σ_a , is resembled as $\sigma_a = (\sigma_{\max} - \sigma_{\min})/2$.

The low-cycle fatigue tests revealed close results for the specimens welded with a rotation speed of 1600 rpm and welding speeds of 100, 200 and 400 mm min⁻¹. The following facts can be deduced by examining the fracture surface of condition B (1600 rpm and 100 mm min⁻¹) by SEM, which has the highest tensile properties among the three conditions.

Cracks initiate and propagate from the imperfections at the root part or the FS markings at the surface of the FS welds. Possible crack initiation sites, indicated with arrows in Figs. 13a,b, originate from the FSW markings on the surface and imperfections in the root part of the FS welds, respectively. Dickerson and Przydatek defined the root imperfections in FS welds as “root flaws” and have provided the feature of root flaws in their paper [20]. The fatigue zone shows cleavage fracture, Fig. 13c, which is reversing into a ductile cracking in the fracture zone. Fatigue propagation exhibits a stable crack growth with relatively smooth areas containing periodic fatigue propagation markings as seen in Fig. 13d.

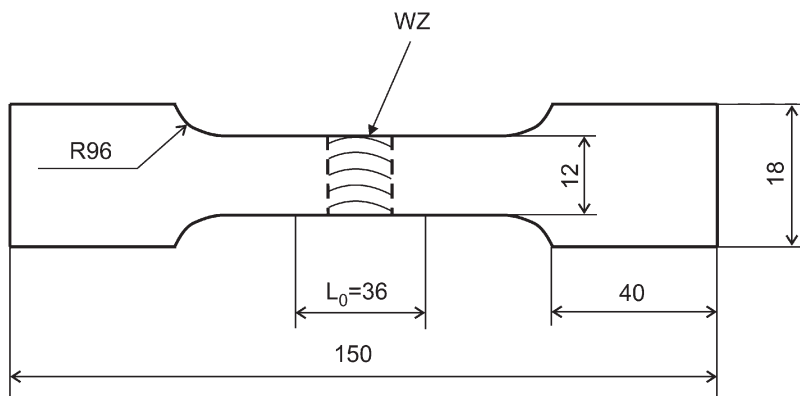


Fig. 11. Schematic of low-cycle fatigue specimen.

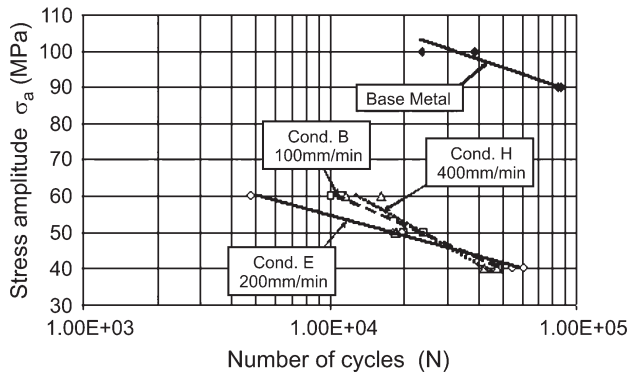


Fig. 12. Low-cycle fatigue life for AA 6063 welded FSW by the welding conditions B, E and H.

4. Conclusions

AA 6063 sheets are friction stir welded as butt joints and tested for various properties. The following results have been obtained:

1. FSW was performed for various welding parameters obtained by changing the rotation and the welding speeds. Void-free and void containing welds were obtained depending on the weld parameters.

The optimum weld parameters were found to be at a rotation speed of 1600 rpm for a welding speed of 100 mm min^{-1} .

2. Smaller grain sizes were obtained due to recrystallization in the nugget region after welding and a homogeneous structure has been detected.

3. The tensile properties of the joints are lower than those of the base material. The welding parameters have significant effects on the tensile properties and fracture locations of the joints. In terms of tensile properties, at an optimum welding speed of 100 mm min^{-1} and rotation speeds 2800 rpm and 1600 rpm, the ultimate strengths of the joints were about 70 % of the base material strength. Yield strength values of the welded specimens are much lower than the yield strength of the BM (about 40 % of the BM value). It has been seen that variation of the weld parameters did not significantly affect the yield strength.

4. The fatigue behaviour of specimens welded under a rotation speed of 1600 rpm and welding speeds of 100 mm min^{-1} and 400 mm min^{-1} exhibited similar behaviour. Fatigue failure always occurred within the weld zone. In the as welded specimens, possible fatigue crack initiation sites were the FS markings on the surface of the weld or imperfections in the weld root.

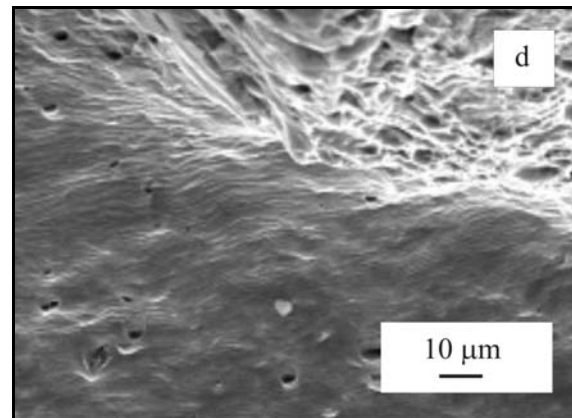
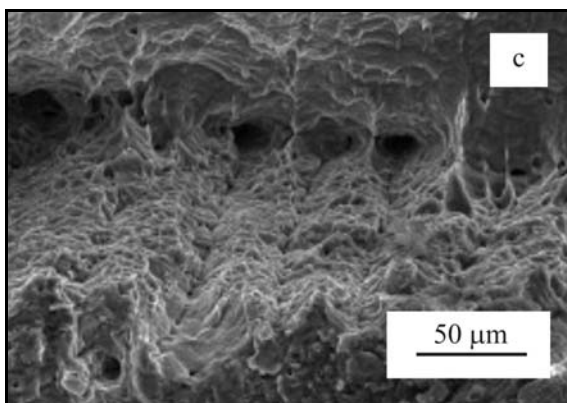
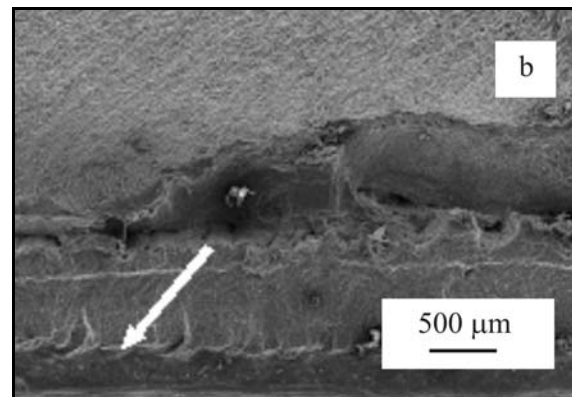
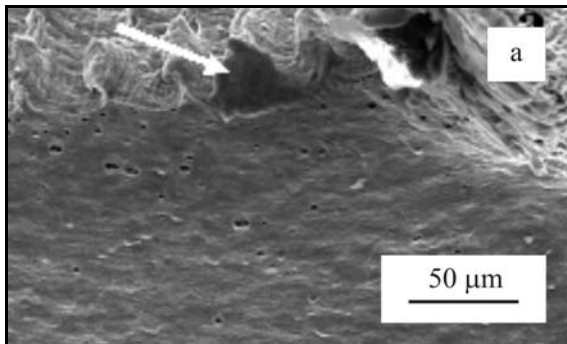


Fig. 13. SEM images of FSW surfaces for condition B (1600 rpm , 100 mm min^{-1}), arrows indicate possible crack initiation sites.

References

- [1] CAVALIERE, P.—NOBILE, R.—PANELLA, F. W.—SQUILLACE, A.: *International Journal of Machine Tools & Manufacture*, 46, 2006, p. 588.
- [2] NICHOLAS, E. D.—KALLEE, S.W.: *Biuletyn Instytutu Spawalnictwa*, 2001, 3, p. 30.
- [3] LAHTI, K.: *Svetsaren*, 58, 2003, p. 6.
- [4] ERIKSSON, L. G.: *Svetsaren*, 56, 2001, p. 3.
- [5] KÜLEKÇİ, M. K.: *Kovove Mater.*, 41, 2003, p. 6.
- [6] THOMAS, W. M.—NICHOLAS, E. D.: *Materials & Design*, 18, 1997, p. 269.
- [7] ERICSSON, M.—SANDSTRÖM, R.: *International Journal of Fatigue*, 25, 2003, p. 1379.
- [8] ZHOU, C.—YANG, X.—LUAN, G.: *Scripta Mater.*, 53, 2005, p. 1187.
- [9] CZECHOWSKI, M.: *Journal of Materials Processing Technology*, 164–165, 2005, p. 1001.
- [10] LOMOLINO, S.—TOVO, R.—DOS SANTO, J.: *International Journal of Fatigue*, 27, 2005, p. 305.
- [11] MISHRA, R. S.—MA, Z. Y.: *Materials Science and Engineering*, R 50, 2005, p. 1.
- [12] SATO, Y. S.—KOKAWA, H.—ENMOTO, M.—JOGAN, S.: *Metall. Mater. Trans.*, A30, 1999, p. 2429.
- [13] KAYALI, E. S.—ENSARİ, C.—DİKEÇ, F.: *Mechanical Tests for Metallic Materials* (in Turkish). Istanbul, Istanbul Technical University Press 1983.
- [14] STARON, P.—KOÇAK, M.—WILLIAMS, S.—WESCOTT, A.: *Physica*, B350, 2004, p. 491.
- [15] MURR, L. E.—LI, Y.—FLORES, R. D.—TRILLO, E. A.: *Mater. Res. Innovat.*, 2, 1998, p. 150.
- [16] LI, Y.—MURR, L. E.—MCLURE, J. C.: *Mater. Sci. Eng.*, A 271, 1999, p. 213.
- [17] MAHONEY, M. W.—RHODES, C. G.—FLINTOFF, J. G.—SPURLING, R. A.—BINGEL, W. H.: *Metall. Mater. Trans.*, A 29, 1998, p. 1955.
- [18] MAHONEY, M. W.—MISHRA, R. S.—NELSON, T.—FLINTOFF, J.—ISLAMGALIEV, R.—HOVANSKY, Y.: *Proc. of Friction Stir Welding and Processing*. Eds.: Yata, K., Mahone, M., Mishra, R. Warrendale, USA, TMS 2001, p. 183.
- [19] SALEM, H. G.: *Scripta Mater.*, 49, 2003, p. 1103.
- [20] DICKERSON, T. L.—PRZYDATEK, J.: *International Journal of Fatigue*, 25, 2003, p. 1399.